Available online at www.sciencedirect.com
ScienceDirect
Journal of the European Ceramic Society 27 (2007) 1927–1933
www.elsevier.com/locate/jeurceramsoc

The application of automated image analysis to dense heterogeneities in partially sintered alumina

Orhan Dengiz [a], Richard McAfee [b], Ian Nettleship [b,*], Alice E. Smith [a]

[a] *Department of Industrial and Systems Engineering, Auburn University, Auburn, AL 36849, USA*
[b] *Department of Materials Science and Engineering, University of Pittsburgh, Pittsburgh, PA 15261, USA*

Received 27 January 2006; received in revised form 10 June 2006; accepted 15 June 2006
Available online 6 September 2006

Abstract

This study used quantitative image analysis to examine the effect of powder forming method on a population of dense heterogeneities that could be imaged in partially sintered alumina using optical microscopy. Powder pressing resulted in a higher area fraction of dense heterogeneities than slip casting. Extreme value analysis was used to predict the size of the largest heterogeneity in the populations and assess the processing methods. Powder pressing resulted in the largest extreme value estimate. The results are interpreted in terms of the effect of the forming method on particle packing and the possible effect of the dense heterogeneities on mechanical strength.

Keywords: Al_2O_3; Pressing; Slip casting; Sintering; Defects

1. Introduction

For ceramics that are derived from powders it has been recognized for some time that microstructure evolution during sintering is spatially heterogeneous, the heterogeneity being derived from the packing of the particles in the green compact.[1] For example, slip casting with dispersed slips has been shown to lead to higher green density and lower sintering temperatures when compared with slip casting using flocculated slips or powder pressing.[2] While the effect of particle packing on densification has been studied several times in terms of the effect of green density on sintering kinetics and the final microstructure,[3–6] there are very few studies that have applied direct measurements of spatial heterogeneity such as two point correlation[7] and pore boundary tessellation.[8]

In addition to studies on the effect of particle packing on green density, it is also recognized that packing can result in a sparse population of larger flaws.[9] These could be associated with: (a) large aggregates resulting from powder preparation,[10] (b) the granulation process,[11] (c) particles of binder that were not properly mixed into the powder during granulation,[12] or (d) large inclusions of a second phase that were intentionally added.[13] It is easy to conclude that a population of relatively large flaws, such as this, could affect material properties such as mechanical strength. Indeed the origins of large flaws have been qualitatively ranked in terms of their expected effect on strength[1] and many of these flaws have been identified at fracture origins. In terms of quantitative understanding, there is only systematic information concerning the effect of some of these defect populations on strength or Weibull modulus.[14] However, this usually involves direct correlations between the processing variables such as granule density and the strength of the sintered ceramics. There has been some direct counting of flaw populations on polished surfaces that result from different forming techniques. This has revealed significant differences that are reflected in the trends in both average strength and Weibull modulus.[15] Mercury porosimetry has also revealed that the forming methods result in measurably different pore size distributions in the green compact,[16] which would correlate with the effect of processing method on strength. In the case of large rigid inclusions, such as reinforcement, there have been more studies because the populations are somewhat higher volume fraction and the reinforcements themselves are easier to identify. This has led to a significant body of modeling,[17–19] concerning the effect of these inclusions on both local and macroscopic densification behavior. Such studies have proved useful in explaining the

* Corresponding author.
E-mail address: nettles@pitt.edu (I. Nettleship).

0955-2219/$ – see front matter © 2006 Elsevier Ltd. All rights reserved.
doi:10.1016/j.jeurceramsoc.2006.06.002

effect of parameters such as the volume fraction of reinforcements on sintering. While little quantitative information exists concerning the spatial distribution of reinforcements in these microstructures it is clear that direct contact between the reinforcements could have an adverse effect on sintering and special measures have been used to avoid such contacts and improve the densification behavior at high loadings of inclusions.[20]

It is apparent that a quantitative understanding of sparse populations of defects in ceramics, whether they result from intentionally added reinforcements or from powder processing, would be useful to our understanding of their effect on the processing and properties of ceramics materials. To this end, the present work was designed to demonstrate a method by which the effect of powder forming method on a sparse population of dense heterogeneities could be quantified. While dense heterogeneities could still be observed in ceramics sintered to solid volume fractions above 0.9, they could easily be identified by optical microscopy in partially sintered alumina ceramics at solid volume fractions ranging from 0.7 to 0.9. Therefore, examination of the dense heterogeneities in partially sintered materials was undertaken.

It would not be unreasonable to suspect that such dense heterogeneities might act as large inclusions in the later stages of densification and result in strength controlling defects as the surrounding matrix attempts to densify onto them. This study assumed that the observed polished sections are a random sampling plane through a representative volume. A similar assumption is implicit in the determination of particle size distributions from microstructural sections. The measured quantities included averages such as area fraction as well as size distributions and the first application of extreme value analysis to assess the powder forming methods. If the largest heterogeneities in the population affect the strength of alumina ceramics then the ranking from the extreme value analysis should agree with previous reports of the effect of forming method on strength.[21]

2. Experimental procedures

Samples of an alumina powder (Alcoa, Premalox, Pittsburgh, PA) were prepared from the same powder batch by three different forming methods: powder pressing, slip casting with a dispersed slip and slip casting with a flocculated slip. The powder had a surface area of 11.6 m^2/g and an average particle size of 0.2 μm. The powder used for pressing was ungranulated and did not contain binder. Uniaxial pressing under 55 MPa resulted in a green density of 57%. The slip cast samples were made with slips containing 20 vol% solids. In the case of the dispersed samples, 50 g of powder was added to deionized water containing 1.7 ml of ammonium polyacrylate dispersant (Darvan C, R.T. Vanderbilt Company). For the slip cast samples made with flocculated slip the 50 g of alumina powder were added to deionized water that had been adjusted to pH 9 with ammonium hydroxide. The samples from both slip conditions were cast in a plaster mold and allowed to dry in room air for approximately 7 days. The green density of the samples could not be measured directly because the dried green samples were not a regular shape. However, green density measurements of samples made using the same method and the same powder as a previous study yielded a value of 55% for the flocculated condition and 62% for the dispersed condition.[22]

All samples, including the pressed samples and the slip cast samples prepared with dispersed and flocculated slips were then sintered at 1350 °C for 0.1 or 0.5 h using a heating rate of 5 °C/min and a cooling rate of 10 °C/min. The solid volume fraction of the samples was measured using the Archimedes method, in which the samples were placed in vacuum prior to being weighed suspended in water. The object of the partial sintering was to get all the samples into the solid volume fraction range (0.7–0.9) in which the dense heterogeneities could be observed by optical microscopy. Given the different sintering kinetics of the samples processed using the different forming methods, the decision was made to compare the populations of heterogeneities after the same sintering times. More limited comparisons could be made at the same solid volume fraction. In order to observe the grain structure the samples were thermally etched at 1325 °C for 18 min using a heating rate of 5 °C/min and a cooling rate of 10 °C/min. This treatment did not affect the solid volume fraction of the samples. For the purpose of clarity, the slip cast samples cast with the slip in the dispersed condition shall be referred to as the "dispersed samples" and the specimens made with flocculated slip will be called the "flocculated samples". Those samples prepared by powder pressing will be called the "pressed samples".

After sintering the samples were sectioned and impregnated with a low viscosity resin to avoid pull-out during section preparation. The sections were subsequently ground flat with 30 μm diamond and pre-polished with 15 μm diamond before polishing with 6 and 1 μm diamond. All polished surfaces were observed using optical microscopy at ×100 using the same illumination conditions. These conditions were chosen so that dense heterogeneities exhibited bright contrast in comparison to the less dense matrix for which the pores could not be resolved, but did cause scattering of the light resulting in darker contrast. Between 10 and 15 images were recorded at randomly chosen positions on the surface of each sample and the approximate positions on the surface was recorded. There appeared to be no correlation between the locations of the images on the section and the population of the dense heterogeneities. The samples' sections were also observed at higher magnification by scanning electron microscopy to observe the dense heterogeneities and their internal grain structure.

Image processing began with thresholding of the dense heterogeneities, which was performed using Scion Image software (http://www.scioncorp.com). Unfortunately the brightness variation between the images or even within an image, combined with the difficulties encountered in focusing on the surfaces made it almost impossible to recover these features using a preset threshold or a density slice technique with fixed parameters. Therefore an adaptive thresholding algorithm[23] was designed to automatically enhance the processed images and set the necessary density slice parameters for recovery of the dense heterogeneities. The goal of this automated process was to eliminate operator error, or variation, which is inevitable if the images

are processed manually. First, a sample batch was taken from the entire population of images and the recovery of the features of interest was done manually, while recording the density slice parameter values. This was followed by regression analysis to develop an estimation function for the best density slicing parameters. The input or independent variables were the average, standard deviation, minimum and maximum of the gray levels and the output variables were the density slice limits. Feature recovery was concluded by a final noise reduction. An example of an optical micrograph showing the brighter, dense heterogeneities is shown in Fig. 1(a). Thresholding with a preset grey level gave a very noisy processed image as shown in Fig. 1(b). The results of manual image processing and the automated image processing method developed in this study are compared in Fig. 1(c and d). Statistical analysis of the results included determination of the area fraction of the dense heterogeneities and their size distribution. No attempt was made to unfold the heterogeneity size distribution into three dimensions. In the analysis it was assumed that the polished surface of each sample is a random section through the material and the images are cumulatively representative. Again, it is worth mentioning that there was no evidence of systematic variations in the population of dense heterogeneities on the polished surfaces. The largest dense heterogeneity in the material was estimated using the generalized Pareto distribution (GPD) which is frequently used to model the tail of distributions and estimate the extreme value.

The Pareto law with a shape parameter γ, scale parameter s, and a location parameter ν can be stated as:

$$1 - F_x(x) = Pr\{X > x\} = \left(\frac{x-\nu}{s}\right)^{-1/\gamma}, \quad \gamma > 0, x \geq \nu \tag{1}$$

Pickands showed, for a large class of underlying distribution functions, that the distribution function, $F_u(y)$, of values of X over a certain threshold u is well approximated by the GPD, for large u.[24] Dargahi–Noubary recommends GPD for use as the distribution of the excess of observed values over a certain threshold, as the threshold increases toward the right hand tail.[25] The GPD is a flexible and widely applied limit distribution that has been applied to modeling high risks in financial markets,[26] earthquake magnitudes,[27] heavy winds,[25,28,29] floods,[24] particle size distributions,[30] and maximum inclusion size in clean steels,[31–34] to name only a few examples. Gilli and Kellezi have provided detailed information on the GPD,[26] from which Eqs. (2) to (3) can be derived.

$$F_u(y)\, G_{\xi\sigma}(y), \qquad u \to \infty$$

$$P(Y \leq y | Y > 0) = G_{\xi,\sigma}(y) = \begin{cases} 1 - \left(1 + \dfrac{\xi}{\sigma} y\right)^{-1/\xi} & \text{if } \xi \neq 0 \\ 1 - \mathrm{e}^{-\xi/\sigma} & \text{if } \xi = 0 \end{cases} \tag{2}$$

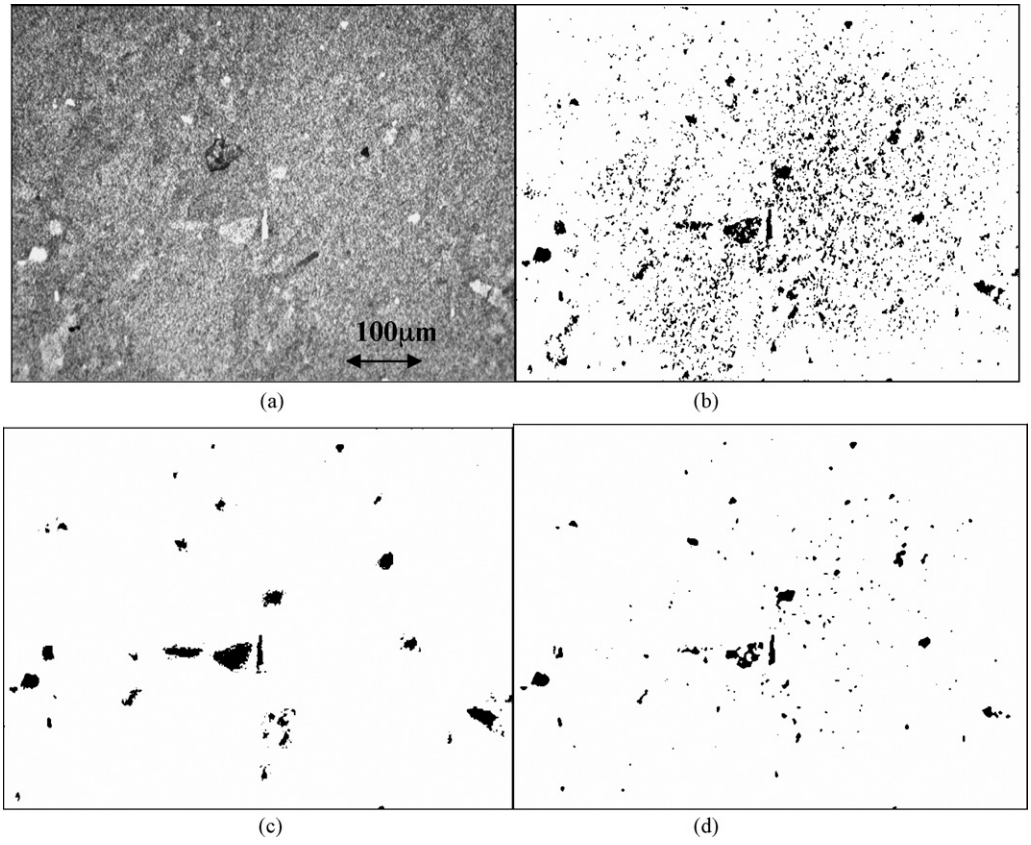

Fig. 1. (a) An example of an optical micrograph where the dense heterogeneities are brighter than the surrounding matrix. (b) The noise that results from thresholding with a fixed grey level, (c) the effects of manual cleaning and thresholding, and (d) the results of the automatic image processing process developed in this study.

Table 1
The effect of processing condition and sintering time on the solid volume fraction (V_s) of the material and the area fraction (AF) of dense heterogeneities

Method	Pressed		Flocculated		Dispersed	
Duration (h)	0.1	0.5	0.1	0.5	0.1	0.5
Sample size	10	12	14	14	12	14
V_s	0.78	0.84	0.75	0.85	0.82	0.90
AF lower CL[a]	0.0021	0.0157	0.0002	0.0013	0.0012	0.0006
AF average	0.0083	0.0205	0.0004	0.0021	0.0015	0.0009
AF upper CL[a]	0.0146	0.0252	0.0006	0.0030	0.0018	0.0012

The sample size refers to the number of images used.
[a] 95% Confidence intervals.

for $0 \le y \le (x_{max} - u)$, is the generalized Pareto Distribution.

If x is defined as $x = u + y$, the GPD can be expressed as a function of x as:

$$P(X < x|X > u) = F(x) = G_{\xi,\sigma}(x - u) = 1 - \left(1 + \xi\frac{(x-u)}{\sigma}\right)^{-1/\xi} \quad (3)$$

The cases where $\xi > 0$, $\xi = 0$, and $\xi < 0$ correspond to Frechet, Gumbel and reverse Weibull domains of attraction, respectively.[27–29] If there is theoretical or scientific evidence that there is a certain upper bound for x, then $\xi < 0$ is used, else $\xi > 0$ is used for applications where there is no knowledge or evidence about the upper limit. Eqs. (2) and (3) are the conditional cumulative distribution of excess $Y = X - u$ given $Y > 0$ or X given $X > u$, respectively, for a sufficiently large threshold u.

3. Results

Fig. 2 shows a dense heterogeneity observed in the scanning electron microscope after thermal etching to reveal the grain boundaries. This clearly shows that the heterogeneities are dense and polycrystalline and the grain size does appear to be larger than the grain size in the surrounding regions, which are more porous. The solid volume fractions of the samples are shown in Table 1 along with the area fractions occupied by the dense heterogeneities and its 95% confidence interval.

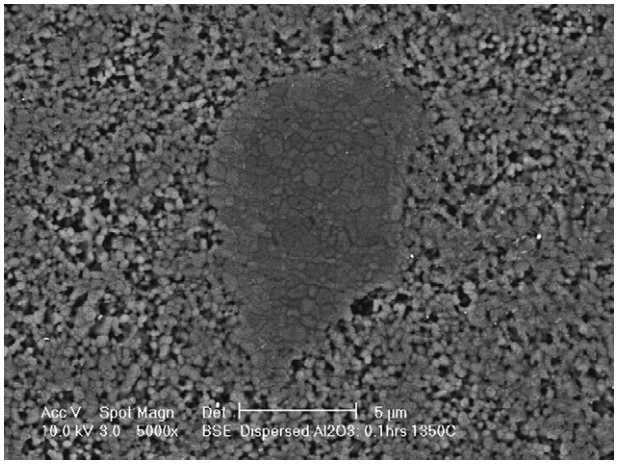

Fig. 2. A dense heterogeneity showing the internal grain structure.

The fraction of the surface occupied by the heterogeneities is relatively low, with the number of heterogeneities per image ranging from a high of 138 for a pressed sample to as low as 11 for the dispersed samples. In the samples sintered for 0.1 h the area fraction of the dense heterogeneities was 0.008 for the pressed sample, which was almost an order of magnitude higher than the area fraction of heterogeneities in the dispersed sample and the flocculated sample. Comparison of the confidence intervals also shows a comparatively large variability for the pressed sample compared to the slip cast samples for the image size used in the optical microscopy. When the sintering time was increased to 0.5 h the area fraction of heterogeneities of the pressed and flocculated samples showed a significant increase that caused the average values to more than double. In comparison, there was no significant difference for the dispersed samples sintered for 0.1 and 0.5 h when the 95% confidence intervals are considered. The results suggest that the fraction of dense heterogeneities increase as the sintering time and the solid volume fraction of the samples increase for the flocculated and the pressed sample thereby suggesting that the population of heterogeneities is changing for these materials. It is also interesting that the increase in sintering time gives much the same change in solid volume fraction (0.75–0.85) for the flocculated and the pressed samples but the dispersed samples sinters over a higher solid volume fraction range (0.82–0.9). To compare the area fraction of heterogeneities for the three processing conditions at approximately the same solid volume fractions the values for dispersed sample sintered for 0.1 h can be compared with the values for the pressed and flocculated sintered for 0.5 h. The comparison shows that the area fractions for the dispersed and the flocculated samples are an order of magnitude less than the area fraction for the pressed material. In summary, it is clear that the area fraction of heterogeneities in the pressed material is much larger than the flocculated or the dispersed material. To determine if the difference in area fraction is associated with a difference in size of the dense heterogeneities it is necessary to consider the size distributions of the heterogeneities.

Fig. 3(a and b) show the number frequency size distributions of heterogeneities in materials sintered for 0.1 and 0.5 h. The flocculated sample appears to have smaller heterogeneities after sintering for 0.1 h compared to the dispersed and the pressed samples. After sintering for 0.5 h the size distribution in the flocculated material is similar to that of the dispersed and the pressed material which is little changed from 0.1 h. This sug-

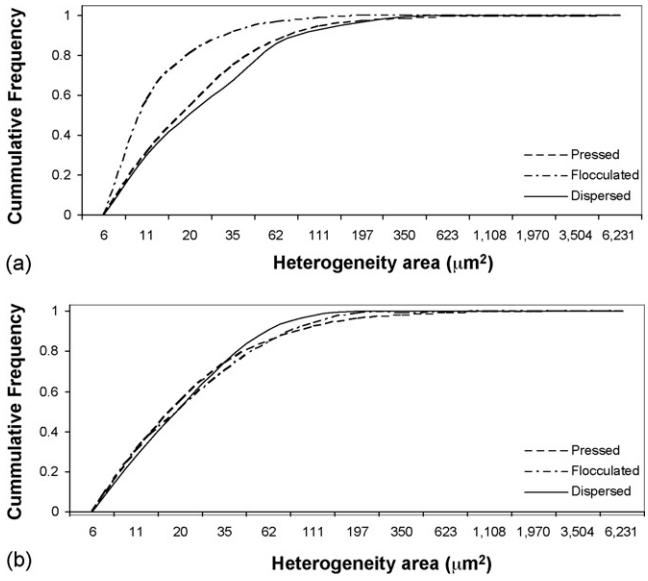

Fig. 3. (a) The number frequency size distribution of dense heterogeneities in materials sintered for 0.1 h at 1350 °C. (b) The number frequency size distribution of dense heterogeneities in materials sintered for 0.5 h at 1350 °C.

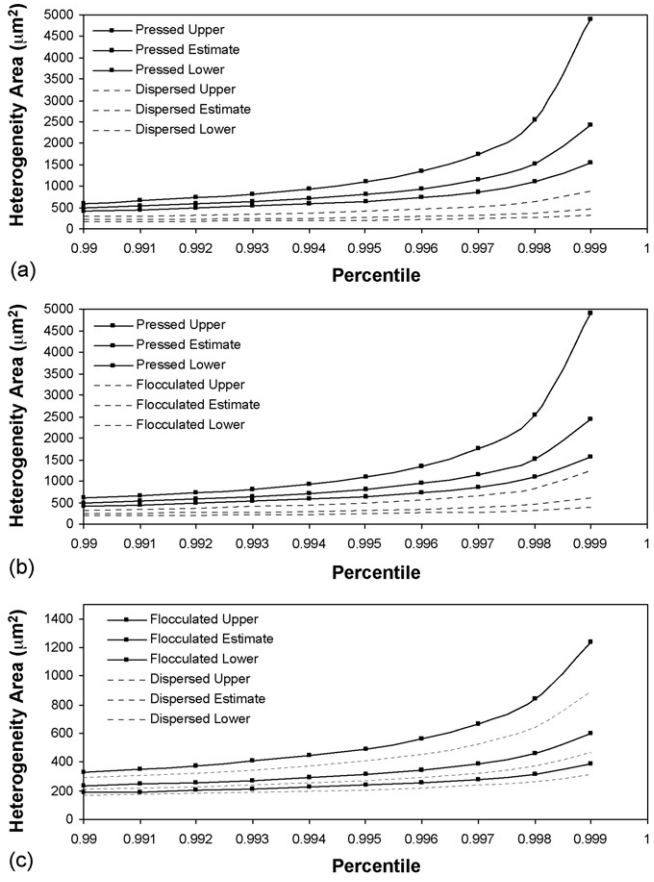

Fig. 4. (a) Percentile plot comparisons for the extreme value of the size of the dense heterogeneities in the pressed and dispersed samples. (b) Percentile plot comparisons for the extreme value of the size of the dense heterogeneities in the pressed and flocculated samples. (c) Percentile plot comparisons for the extreme value of the size of the dense heterogeneities in the flocculated and dispersed samples.

gests that the dense heterogeneities in the flocculated material change in size. However, the previously described changes in area fraction for the pressed material is mostly associated with changes in the number of dense heterogeneities.

For the extreme value analysis, the data for both sintering times was combined to compare predictions for the pressed, dispersed and flocculated materials. Estimates were determined for the maximum sizes of the dense heterogeneities at 40 different percentile values. Percentile plots for the three different processing methods are compared in Fig. 4(a–c). Each of these predictions shows an average value for each percentile and an upper and lower prediction based on the 90% confidence interval. Fig. 4a and b show that the results for the pressed samples can be separated from the predictions of the dispersed and the flocculated. Clearly the predicted area of the largest heterogeneity in the pressed sample is larger than that for the dispersed or the flocculated samples. For example, the area of the heterogeneity at the 99.9 percentile is 2434 μm^2 for the pressed sample, which is four to five times the value of the flocculated (598 μm^2) and dispersed material (465 μm^2) at the same percentile. Fig. 4c shows that the prediction is higher for the flocculated material than the dispersed materials, however, the difference is not significant compared to values of the 90% confidence intervals.

4. Discussion

While the qualitative observation of the dense heterogeneities in partially sintered materials was straight forward due to their high reflectivity, the quantitative determination of the population is somewhat more difficult. It requires the assumption that the polished section is equivalent to a random plane through a volume that is representative and contains no systematic variations in the population. Examination of the population by location on the polished sections did not show any evidence that would call these assumptions into question. A greater obstacle to this study was presented by the image processing required to create the binary images for image analysis. It is not unreasonable to expect that partially sintered materials are spatially heterogeneous, containing regions of higher local solid volume fraction. In optical microscopy such variation in solid volume fraction would result in a spatial variation of contrast due to the difference in the amount of light scattering at pores. In this circumstance, a manual threshold of denser areas would depend on what the operator perceived as “dense”. To avoid this ambiguity an automated image processing technique was developed in this study to capture only the very dense regions with the highest brightness. This allowed for correlations between the processing techniques that were independent of manual image processing conditions. It also resulted in a large reduction in the amount of time required to process and analyze the images. However, it must be remembered that the remainder of the material surrounding the dense heterogeneities is not necessarily uniform in solid volume fraction.

The results of this study have showed that the area fraction of a sparse population of dense heterogeneities was affected by the powder forming method used to shape the powder and by

sintering time. This provides evidence that this is not simply a population of dense heterogeneities that was present in the original powder and remained unaffected by the powder forming technique. It would imply that powder pressing, in particular, results in spatial heterogeneity in the packing of the particles that not only results in lower green density but also promotes the formation of the dense heterogeneities during sintering. The size distribution measurements show that, with the exception of the flocculated material sintered for 0.1 h, there seemed to be little difference between the processing methods used. At this point it is important to remember that the observed populations are dense heterogeneities and not the pore population which has been shown to be sensitive to processing method.[16] From the results of the present study it is possible to conclude that difference in the measured area fractions for the pressed, flocculated and the dispersed materials is associated with differences in the number of heterogeneities per unit area of the polished surface. The pressed material in particular contained a larger number of heterogeneities and more heterogeneities formed at longer sintering times.

Although additions of dense particles at levels as low as 5 vol% have been shown to effect densification kinetics of ceramics during sintering,[35] the dense heterogeneities observed in this study are present in very small fractions and it is unlikely that they will have much effect on average properties such as the bulk densification rate during initial and intermediate stage sintering. However, they may correlate with a significant fraction of the pores remaining towards the end of final stage sintering and thereby affect kinetics. There have been many studies on sintering in the presence of dense inclusions,[17–19] that would suggest such heterogeneities would constrain the sintering shrinkage of the surrounding material and may well result in a defect in the final sintered material. In this circumstance the strength of the ceramics might be controlled by the largest heterogeneity in the population. Therefore the extreme value analysis undertaken in this study could be used to generate a ranking of the processing methods that should correlate with the effect of the processing method on the strength and Weibull modulus of the alumina ceramics. While a direct comparison with mechanical properties is beyond the scope of this study, the general conclusion does agree with the effect of processing condition on strength from previous studies which showed that processing using colloidal methods gave higher strength than powder pressing.[21]

5. Conclusions

This study has showed that quantitative image analysis can be applied to comparatively large, dense heterogeneities that develop during the sintering of ceramics. The population of dense heterogeneities in partially sintered material was found to depend on both the powder forming method and the sintering condition. In particular the area fraction of dense heterogeneities and the largest heterogeneity in the size distribution, estimated using extreme value analysis, were appreciably higher for the pressed material in comparison with slip cast materials made from the same batch of powder.

Acknowledgements

The authors would like to thank the National Science Foundation for funding this project under grant DMI 0301273. The use of the facilities in the Materials Micro-Characterization Laboratory at the University of Pittsburgh is also gratefully acknowledged.

References

1. Lange, F. F., Powder processing science and technology for increased reliability. *J. Am. Ceram. Soc.*, 1989, **72**, 3–15.
2. Yeh, T. S. and Sacks, M. D., Low-temperature sintering of aluminum oxide. *J. Am. Ceram. Soc.*, 1988, **71**, 841–844.
3. Occhionero, M. A. and Halloran, J. W., The influence of green density upon sintering. In *Sintering and Heterogeneous Catalysis, Materials Science Research*, *vol. 16*, ed. G. C. Kuczynski, A. E. Miller and G. A. Sargent. Plenum Press, New York, 1984, pp. 89–102.
4. Cameron, C. P. and Raj, R., Better sintering through green-state deformation processing. *J. Am. Ceram. Soc.*, 1990, **73**, 2032–2037.
5. Rahaman, M. N., De Jonghe, L. C. and Chu, M. Y., Effect of green density on densification and creep during sintering. *J. Am. Ceram. Soc.*, 1990, **74**, 514–519.
6. Chen, P.-L. and Chen, I.-W., Sintering of fine oxide powders: I, microstructure evolution. *J. Am. Ceram. Soc.*, 1996, **79**, 3129–3141.
7. Missiaen, J. M. and Chaix, J. M., The homogeneity of phase repartition in TiB_2–Fe composites using variance and covariance analysis. *J. Microsc.*, 1994, **175**, 195–204.
8. McAfee, R. J. and Nettleship, I., A mesoscale description of microstructure evolution for the sintering of ceramics. *Acta Mater.*, 2005, **53**, 4305–4311.
9. Lange, F. F. and Metcalf, M., Processing-related fracture origins: II, agglomerate motion and crack-like internal surfaces caused by differential sintering. *J. Am. Ceram. Soc.*, 1983, **66**, 398–409.
10. Rhodes, W. H., Agglomeration and particle size effects on sintering yttria-stabilized zirconia. *J. Am. Ceram. Soc.*, 1981, **64**, 19–22.
11. Frey, R. G. and Halleron, J. W., Compaction behavior of spray dried alumina. *J. Am. Ceram. Soc.*, 1984, **67**, 199–203.
12. Lange, F. F., Davis, B. I. and Wright, E., Processing-related fracture origins: IV, elimination of voids produced by organic inclusions. *J. Am. Ceram. Soc.*, 1986, **69**, 66–69.
13. Sudre, O. and Lange, F. F., Effect of inclusions on densification: I, microstructural development in a Al_2O_3 matrix containing a high volume fraction of ZrO_2 inclusions. *J. Am. Ceram. Soc.*, 1992, **75**, 519–524.
14. Walker, W. J., Reed, J. S. and Verma, S. K., Influence of granule character on strength and Weibull modulus of sintered alumina. *J. Am. Ceram. Soc.*, 1999, **82**, 50–56.
15. Huisman, W., Graule, T. and Gauckler, L. J., Alumina of high reliability by centrifugal casting. *J. Eur. Ceram. Soc.*, 1995, **15**, 811–821.
16. Krell, A. and Klimke, J., Effects of the homogeneity of particle coordination on solid-state sintering of transparant alumina. *J. Am. Ceram. Soc.*, 2006, **89**, 1985–1992.
17. Hsueh, C. H., Evans, A. G. and Cannon, R. M., Viscoelastic stresses and sintering damage in heterogeneous powder compacts. *Acta Metall.*, 1986, **34**, 927–936.
18. Scherer, G. W., Sintering with rigid inclusions. *J. Am. Ceram. Soc.*, 1987, **70**, 719–725.
19. Sudre, O., Bao, G., Fan, B., Lange, F. F. and Evans, A. G., Effect of inclusions on densification: II, numerical model. *J. Am. Ceram. Soc.*, 1992, **75**, 525–531.
20. Hu, C. L. and Rahaman, M. N., Factors controlling the sintering of ceramic particle composites: II coated inclusion particles. *J. Am. Ceram. Soc.*, 1992, **75**, 2066–2070.
21. Kreil, A., Fracture origin and strength in advanced pressureless-sintered alumina. *J. Am. Ceram. Soc.*, 1998, **81**, 1900–1906.

22. Schmidt, S. A., The microstructure of densifying ceramic and metal powders, MS Thesis, University of Pittsburgh, Pittsburgh, PA, 1998.
23. Dengiz, O., Smith, A. E. and Nettleship, I., Two-stage data mining for flaw identification in ceramics manufacture. *Int. J. Prod. Res.*, 2006, **44**, 2839–2851.
24. Pickands III, J., Statistical inference using extreme order statistics. *Ann. Stat.*, 1975, **3**, 119–131.
25. Dargahi-Noubary, G. R., On tail estimation: an improved method. *Math. Geol.*, 1989, **21**, 829–842.
26. Gilli, M. and Kellez, E. I., An application of extreme value theory for measuring financial risk, Research paper. Preprint submitted to *Elsevier Science*, Available online at: http://www.unige.ch/ses/metri/gilli/evtrm/GilliKelleziEVT.pdf, accessed 14 July 2005.
27. Caers, J., Beirlant, J. and Maes, M. A., Statistics for modeling heavy tailed distributions in geology: part I methodology. *Math. Geol.*, 1999, **31**, 391–410.
28. Simui, E. E. and Heckert, N. A., *Extreme Wind Distribution Tails: A'Peaks Over Threshold' Approach, National Institute of Standards and Technology Building Science Series, vol. 174*. Coden: NBSSES, 1995, March.
29. Heckert, N. A., Simiu, E. and Whalen, T., Estimates of hurricane wind speeds by "peaks over threshold" method. *J. Struct. Eng.*, 1998, **124**, 445–449.
30. Dierickx, D., Basu, B., Vleugels, J. and Van der Biest, O., Statistical extreme value modeling of particle size distributions: experimental grain size distribution type estimation and parameterization of sintered zirconia. *Mater. Character.*, 2000, **45**, 61–70.
31. Shi, G., Atkinson, H. V., Sellars, C. M. and Anderson, C. W., Application of the generalized Pareto distribution to the estimation of the size of the maximum inclusion in clean steels. *Acta Mater.*, 1999, **47**, 1455–1468.
32. Anderson, C. W., Shi, G., Atkinson, H. V. and Sellars, C. M., The precision of methods using the statistics of extremes for the estimation of the maximum size of inclusions in clean steels. *Acta Mater.*, 2000, **48**, 4235–4246.
33. Shi, G., Atkinson, H. V., Sellars, C. M., Anderson, C. W. and Yates, J. R., Computer simulation of the estimation of the maximum inclusion size in clean steels by the generalized Pareto distribution method. *Acta Mater.*, 2001, **49**, 1813–1820.
34. Anderson, C. W., Shi, G., Atkinson, H. V., Sellars, C. M. and Yates, J. R., Interrelationship between statistical methods for estimating the size of the maximum inclusion in clean steels. *Acta Mater.*, 2003, **51**, 2331–2343.
35. Tuan, W. H., Gilbert, E. and Brook, R. J., Sintering of heterogeneous ceramic compacts part 1 Al_2O_3–Al_2O_3. *J. Mater. Sci.*, 1989, **24**, 1062–1068.